Product state distributions in the photodissociation of expansion-cooled NO_2 near the $NO(X\,^2\Pi)$ $v=1$ threshold

D.C. Robie, M. Hunter, J.L. Bates [1] and H. Reisler

Department of Chemistry, University of Southern California, Los Angeles, CA 90089-0482, USA

Received 27 February 1992; in final form 24 March 1992

The photodissociation of NO_2 near the NO $v=1$ threshold was studied using a supersonic molecular beam of NO_2 and multiphoton ionization detection of $NO(X\,^2\Pi_{1/2,\,3/2})$. The vibrational populations near the $v=1$ threshold are nonstatistical as compared with the predictions of phase space theory (PST). The rotational distributions in both NO $v=0$ and 1 show pronounced structures and fluctuations; however, their average is described fairly well by PST, suggesting that the decomposition of NO_2 at $\lambda \geqslant 370$ nm can be viewed as vibrational predissociation on the mixed $\tilde{X}\,^2A_1/1\,^2B_2$ surface. Similar structured rotational distributions have been observed by Miller et al. in recent studies of the photodissociation of CO_2 at 157 nm. The structures in the rotational distributions are interpreted as fluctuations inherent in the decomposition of an excited complex with many overlapping resonances (Ericson fluctuations).

1. Introduction

The photodissociation of NO_2 is important both in the understanding of atmospheric chemistry and energetic material decomposition, and as a prototype small molecule whose dissociation is at the crossroads between statistics and dynamics. It is therefore surprising that despite substantial effort, no cohesive picture has yet emerged regarding the mechanism of NO_2 decomposition and its dependence on excess energy, $E^\dagger = E_{photon} - D_0$. In particular, the region near the $v=1$ threshold (350–370 nm) has been the subject of several studies using 300 K samples [1–4]. Welge and co-workers found that the NO vibrational distributions measured with 351 and 337 nm photolyses ($E^\dagger = 3360$ and 4540 cm^{-1}, respectively) are decidedly nonstatistical, and concluded that the rotational distributions are non-statistical as well [1,2]. In contrast, Mons and Dimicoli, who did not measure the vibrational distributions, found that the NO rotational distributions measured with 300 K samples at excess energies from the $v=1$ threshold up to $E^\dagger = 3600$ cm^{-1} ($\lambda \geqslant 348$ nm) are well fit by statistical (prior) distributions [3,4]. A statistical interpretation of the dissociation was first proposed by Troe and co-workers [5,6], who used the statistical adiabatic channel model.

The monoenergetic dissociation rates of NO_2 in this wavelength region have only recently been measured directly, and are $> 2.0 \times 10^{12}$ s^{-1} at excess energies $E^\dagger > 1200$ cm^{-1} [7]. Other studies have shown that the dissociation lifetimes decrease sharply with $E^\dagger$, and at $E^\dagger \geqslant 4500$ cm^{-1} ($\lambda \leqslant 338$ nm), they are shorter than a vibrational period. The lifetimes have been estimated from the photofragment yield spectra [8], resonance Raman spectroscopy [9], and the recoil anisotropy parameters of the fragments [10–12].

The interpretation of the dissociation dynamics of NO_2 is complicated by the strong couplings among its electronic states. In particular, the well-known mixings between the $1\,^2B_2$ and $\tilde{X}\,^2A_1$ states, which arise from a conical intersection, have been investigated extensively both theoretically [13–17] and experimentally [18–23], and are implicated in the spectroscopy and unimolecular decomposition of NO_2. At energies near the dissociation threshold,

Correspondence to: H. Reisler, Department of Chemistry, University of Southern California, Los Angeles, CA 90089-0482, USA.

[1] Present address: Department of Chemistry, Santa Monica College, Santa Monica, CA 90404, USA.

other electronic states (e.g., $1\,^2A_2$, $1\,^2B_1$) may be involved as well [14,19], but considerations of density of states dictate that the molecular eigenstates have a predominantly ground-state character. Based on ab initio calculations and symmetry correlations for *linear* NO_2, it was suggested that the $1\,^2B_2$ state does not correlate with $NO(X\,^2\Pi)+O(^3P)$, but rather with $NO(X\,^2\Pi)+O(^1D)$ [17], but the correlations for the actual bent states might be different. Nevertheless, experimental evidence (e.g., rates, structured spectra, etc.) suggests that near threshold, decomposition evolves mainly on the ground electronic state. On the other hand, the strong nonadiabatic forces acting near the conical intersection give rise to fast changes of the adiabatic states with the nuclear coordinates in the vicinity of the intersection [13]. Therefore, the nuclear behavior in this region may be complicated and affect the dynamics.

By optically exciting the $1\,^2B_2$ state, it is possible to efficiently prepare monoenergetic ensembles of NO_2 molecules with a large ground-state character that dissociate when the photon energy exceeds D_0 (25 130 cm^{-1} [8,24,25]). Although we regard the decomposition of NO_2 at $E^{\dagger}=0$–2000 cm^{-1} as vibrational predissociation, the use of statistical theories to interpret the data should be viewed with caution. The existence of only three vibrational degrees of freedom and strong couplings among the electronic state require that even such basic tenets of statistical theories as the reaction coordinate, transition state, intramolecular vibrational redistribution (IVR) and density of dissociative states be examined carefully. Thus, the question whether the dissociation of NO_2 can be treated within the framework of statistical theories is not a simple one.

In this paper, we report our preliminary results on the product vibrational and rotational state distributions obtained in the vicinity of the $NO(v=1)$ threshold by using molecular beam of expansion-cooled NO_2 ($T_{rot}=7\pm5$ K). By reducing the averaging over the initial parents states, we hope to make the comparisons with statistical theories more rigorous. In addition, with our experimental procedure, we minimize the amount of background NO, thus enabling us to obtain distributions in both $v=0$ and 1. Our results show that already near the threshold of $v=1$, the vibrational populations are nonstatistical. The rotational distributions are structured and show fluctuations about their average which, in turn, is well described by phase space theory (PST). The results are discussed in terms of a unimolecular reaction involving strongly coupled electronics states.

2. Experimental

NO_2 in a pulsed, supersonic molecular beam was photodissociated using one-photon laser excitation, and the resulting NO product monitored with 1+1 resonance-enhanced multiphoton ionization (REMPI). The molecular beam was composed of a mixture of 3% NO_2 and 3% O_2, made up to a total pressure of 700 Torr with He. (O_2 was added to reduce contaminant NO [26].) The gas mixture was expanded through a 0.25 mm diameter nozzle, operated at 10–20 Hz with a piezoelectric valve [27]. The beam was skimmed in a differentially pumped region into a high vacuum chamber (1×10^{-7} Torr), yielding NO_2 rotational temperatures of 7 ± 5 K at the interaction region (10 cm from the nozzle orifice). These temperatures were estimated from the rotational structures in the $NO(v=0)$ photofragment yield spectra to the red of D_0; no signal originating from the $NO_2(010)$ level was observed.

The output of an excimer-pumped dye laser (Lambda-Physik EMG201/FL3002) was used for the NO_2 photolysis (360–380 nm). Typical pulse energies were 1–10 mJ, and the beam was kept unfocused to prevent two-photon dissociation of NO_2. The NO product was probed by 1+1 REMPI via the NO $\gamma(0,0)$ and $\gamma(1,1)$ bands of the $A\,^2\Sigma^+\leftarrow X\,^2\Pi$ transition at 223–226 nm; these wavelengths were obtained by frequency-doubling the output of a similar excimer/dye laser system with a BBO crystal. The probe laser beam was counterpropagated with the photolysis laser, and delayed by 100–300 ns. With $[NO_2]\approx10^{12}$ cm^{-3} at the interaction region, it was possible to eliminate the effects of intra-beam collisions of the NO photofragments prior to ionization. A 100 cm focal-length lens was used to slightly focus the probe beam in the interaction region. Typical probe laser energies were 5–10 μJ/pulse, which resulted in partial saturation of the NO γ bands. Both photolysis and probe laser energies were monitored with photodiodes on a shot-to-shot basis, and used for normalizing the NO^+ ion signals. (Photolysis

pulse energies were not strongly wavelength dependent over the tuning range used, but probe pulse energies dropped by as much as a factor of 2 from the low to the high frequency ends of the REMPI spectrum.) The NO^+ ions were accelerated by a Wiley–McLaren time-of-flight mass spectrometer onto a microchannel plate detector (Galileo; gain $\approx 10^7$). The resulting signal was further amplified ($\times 10^2$) and recorded in a computer through a transient digitizer (LeCroy 8818A; 10 ns resolution).

The experiment was performed in a supersonic molecular beam for two reasons. First, by expansion-cooling the gas mixture to ≈ 10 K, we greatly reduced the possibility of any nonstatistical product state distributions being averaged out by too broad a parent rotational state distribution. Second, we wanted to minimize the contribution from contaminant NO to the REMPI signals. Seeding the NO_2/He with O_2 kept the contaminant NO density less than 14% of the NO density resulting from photolysis, while cooling the contaminant NO to < 5 K ensured that only levels with $J'' \leqslant 2.5$ had any significant population. Thus, it was possible to greatly improve upon previous NO_2 photolysis experiments carried out at 300 K. (NO contamination prevented complete analyses of the NO $v=0$ product channel in some earlier studies [4]. The data were collected with the pump beam alternately "on" and "off" in order to subtract the contaminant NO REMPI signal from that of NO_2 photolysis products.

At the pulse energies and focusing conditions used with the probe laser, we observed partial saturation of the stronger NO rotational branches of the $\gamma(0, 0)$ band (e.g., the unresolved R_1+Q_{21} and Q_1+P_{21} branches) in our REMPI spectra. It was necessary to correct for this effect in extracting NO rotational state populations from these spectra. To this end, we obtained a 1+1 REMPI spectrum of 300 K NO over the $\gamma(0, 0)$ band at the same laser pulse energies and focusing conditions, and deduced normalizing factors by matching the total integrated intensities of the stronger branches to those of the weaker, unsaturated ones. Despite the crudeness of this approach [28], it only introduced a 10% error in deriving rotational temperatures from the 300 K NO sample [29].

The NO γ-band rotational branches in our REMPI spectra were assigned in accordance with previous studies [30]; overlapping peaks, including peaks in the bandheads, were excluded from the rotational analysis. In obtaining NO rotational populations, we normalized the 1+1 REMPI signals to the probe laser pulse energy. (Dividing by the square of the probe laser pulse energy did not substantially affect the relative rotational populations within each branch.) Isolated peaks were integrated around the maximum, and then divided by their line strengths and by the saturation normalizing factor for that branch (0.7 for the stronger branches; 1 for the weaker ones). No correction for alignment effects were made, since the rotational alignment at the dissociation energies used in this study is negligible [4]. When several lines could be identified originating from the same J'', their populations were averaged.

To obtain NO($v=0$, 1) vibrational distributions, we simply divided the 1+1 REMPI signals by the probe pulse energy, and integrated over the entire band. With the NO rotational excitation observed, the $\gamma(0, 0)$ and $\gamma(1, 1)$ bands had negligible overlap. The integrated band intensity from the contaminant NO, exclusively in the $\gamma(0, 0)$ band and obtained simultaneously as described in the last section, was subtracted from the total $\gamma(0, 0)$ band intensity. The band intensity of the contaminant NO was 1%–14% of the total $\gamma(0, 0)$ band intensity. Finally, the band intensities were divided by the Franck–Condon factors [31].

In order to make sure that the partial saturation of the strong branches in the $\gamma(0, 0)$ did not affect these results, we also summed the relative rotational populations for each band. Levels in $v=0$ for which no population could be obtained (due to overlapped lines) were neglected, but by interpolation they contributed no more than 10% to the $v=0$ population. The sums of the relative rotational populations were divided by the Franck–Condon factors, as before. This procedure gave the same results as the other.

The error estimates include the differences between the results of the two methods of data analysis; the effect of normalizing by the first or second power of the probe energy; and the scatter among replicated measurements.

The photolysis laser wavelength was calibrated by collecting 2+1 REMPI spectra of jet-cooled NO samples over the spectral region 365–391 nm. By comparing the spectra with previously published ex-

perimental information [32], we were able to identify five NO bands from the A–X, B–X, and C–X transitions to be used in the calibration. It was thus possible to determine the NO_2 photolysis energies to within 2 cm^{-1}.

The gases used were NO_2 (Matheson, >99.5%), purified by freeze–thaw cycles in a dry ice/acetone slush bath, and O_2 (Spectra Gases, 99.99%) and He (MG, 99.999%), which were used without further purification.

3. Results

NO product state distributions were measured at two photolysis wavelengths, 369.17 and 368.51 nm, corresponding to 73 and 122 cm^{-1} above the threshold for $O(^3P_2)+NO(^2\Pi_{1/2}, v=1)$ production ($E^\dagger=1949$ and 1998 cm^{-1} respectively). Fig. 1 shows a photofragment yield spectrum obtained by monitoring the $NO(^2\Pi_{1/2}, v=1, J=0.5)$ ion signal while scanning the pump laser through the $NO(v=1)$ threshold. The spectrum indicates the onset of photofragmentation at $D_0+E^\dagger=27006$ cm^{-1}, thus placing an upper limit to any barriers to dissociation of <2 cm^{-1} (our experimental uncertainty in photolysis energy). The two photolysis energies are <50 cm^{-1} apart, but sample structurally different regions of the photofragment yield spectrum (points A and B in fig. 1). The structure observed in this spectrum, with irregularly scattered prominent peaks of 10–20 cm^{-1} width, is similar to that observed in a supersonic beam in the $NO(v=0)$ threshold region analyzed by Robra et al. [24], and the photofragment yield spectrum obtained by monitoring $O(^3P_2)$ [8]. For example, the large peak at $D_0+E^\dagger=27075$ cm^{-1} (peak A in fig. 1) has also been observed in ref. [8].

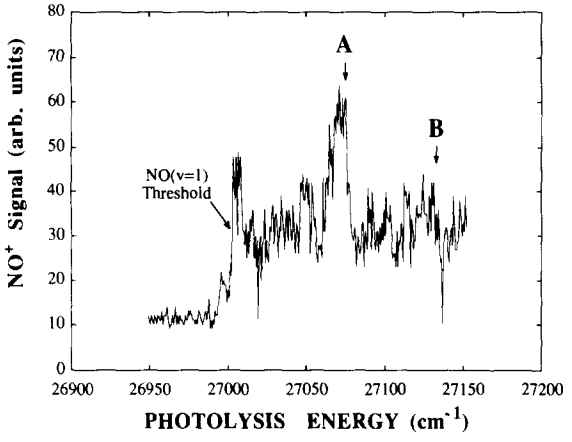

Fig. 1. Photofragment yield spectrum of NO_2 obtained by monitoring $NO(X\,^2\Pi_{1/2}, v=1, J=0.5)$. The $Q_{11}(0.5)$ line was monitored as a function of photolysis laser wavelength.

3.1. Product rotational and vibrational state distributions

Figs. 2 and 3 show the $NO(v=1$ and $0)$ rotational distributions obtained from NO_2 photolysis at the two excess energies indicated in fig. 1 ($E^\dagger=1949$ and 1998 cm^{-1}). It can be seen that in both NO vibrational product channels the rotational populations tend, on average, to follow a statistical distribution predicted from PST [33–36]. However, prominent structures are evident, particularly in the $NO(v=0)$ channel, where adjacent rotational levels commonly show fluctuations beyond our experimental uncertainty and the predictions of PST. In addition, broader structures involving several adjacent levels are observed, which fluctuate significantly around PST expectations and show a sensitive photolysis energy dependence. (Notice the logarithmic scale in fig. 3.) The fluctuations in both $v=0$ and 1 distributions become larger and more random when each Λ-doublet state of each NO spin–orbit state is plotted separately [2,29]. The fluctuations in the $NO(v=1)$ rotational distributions disappear when using 300 K NO_2 samples [1–4], and we conclude that averaging over parent rotational states smoothes over the fluctuations.

The vibrational distributions, on the other hand, cannot be described by PST. Fig. 4 shows the fraction of NO produced in the $v=1$ channel at the two excess energies, and it is apparent that these vibrational distributions are distinctly nonstatistical. The fraction of $NO(v=1)$ is greater than expected by PST, and moreover appear to decrease slightly as the photolysis energy is increased. PST does predict some step-like structures in the excess energy dependence of the $NO(v=1)$ fractional population (reflecting the opening of new dissociation channels), especially around the thresholds for the NO and $O(^3P)$ spin–orbit multiplets. However, these expected steps

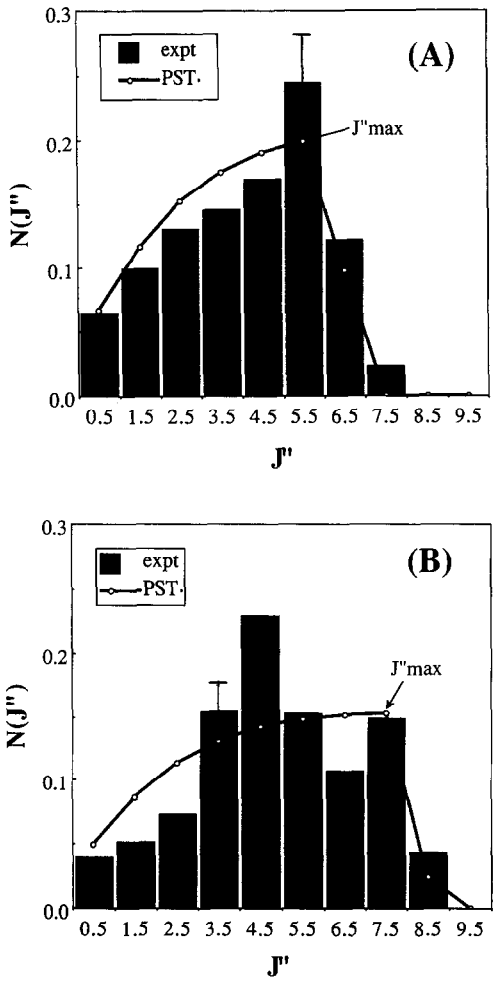

Fig. 2. Rotational populations of NO($X\,^2\Pi_{1/2}$, $v=1$) following dissociation of NO_2 at (A) 369.17 and (B) 368.51 nm. The populations were obtained by correcting for partial saturation and summing over all branches as discussed in the text. The excess energies were computed with respect to the NO($X\,^2\Pi_{1/2}$, $v=1$)+O($^3P_2$) threshold. PST calculations, done at 10 K, are indicated by the smooth curve. J''_{max} marks the highest energetically allowed rotational level for a beam temperature of 0 K.

in the NO($v=1$) fraction cannot account for an apparent decrease with excess energy as shown in fig. 4.

3.2. PST calculations

PST has been a common tool for gauging the statistical nature of product state distributions in unimolecular decay. PST conserves total angular momentum as well as total energy [33–36]:

$$E_{NO_2}+E^{\dagger}=E_t+E_{NO}+E_{O(^3P)}\,, \qquad (1)$$

$$J_{NO_2}=J_{NO}+J_{O(^3P)}+L\,, \qquad (2)$$

where E_i and J_i are the internal energy and the total angular momentum of species i, E_t is the relative

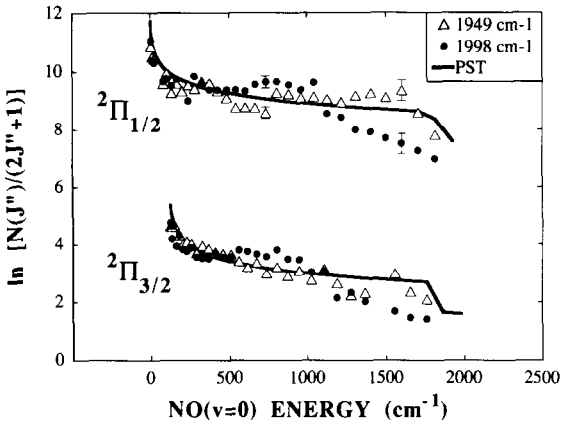

Fig. 3. Rotational populations of NO($X\,^2\Pi_{1/2,3/2}$, $v=0$) following dissociation of NO_2 at 369.17 and 368.51 nm. The populations were obtained as described in fig. 2. Arbitrary constants have been added to the results for each NO spin–orbit state for vertical separation. The excess energy, $E^{\dagger}=1998$ cm^{-1}, was computed with respect to the NO($X\,^2\Pi_{1/2}$, $v=0$)+O($^3P_2$) threshold. The PST calculation at 10 K are indicated by the full curve; (Δ) 1949 cm^{-1}; (●) 1998 cm^{-1}.

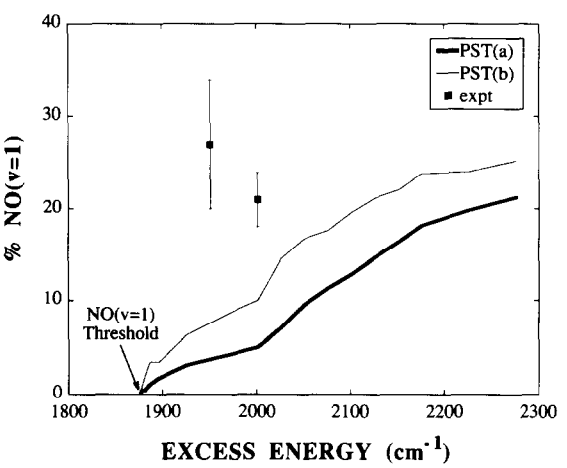

Fig. 4. Measured and calculated (PST) NO vibrational populations. % NO ($v=1$) is the percentage of NO in $v=1$. The PST calculations were carried out assuming a statistical distribution among the O(^3P_J) spin–orbit states (curve a, thick line), or only O($^3P_2$) (curve b, thin line).

translational energy of the photolysis products, and L is the orbital angular momentum of the photofragments. The inclusion of L accounts for the requirement that the fragments have sufficient energy to overcome the L-dependent centrifugal barrier. This results in

$$L(L+1)h^2 \leqslant 24\pi^2\mu C_6^{1/3}(E_t/2)^{2/3}, \quad (3)$$

where one assumes a long-range attractive potential of the form $V(r) = -C_6 r^{-6}$ [37], and μ is the reduced mass of the photofragments. Combining eqs. (1)–(3), one obtains the PST distributions by summing over the available product states in $\{J_{NO}, J_{O(^3P)}, L\}$ space. The theory has been described elsewhere [33–36], and its detailed application to NO_2, as well as comparisons with other statistical theories, will be reported in a forthcoming publication [29].

From the known atomic polarizability of $O(^3P)$ and the dipole moment of NO it is possible to estimate C_6 as 10^{-78} J m^6 [34]. PST predictions of the rotational product state distributions were insensitive to the value of C_6 for low and intermediate J_{NO}. However, calculations using values of $C_6 < 10^{-76}$ J m^6 caused truncation of the rotational distributions at high J (e.g., a value of $C_6 = 10^{-78}$ J m^6 truncates the highest three rotational levels in the NO(v=0) distributions). The agreement between experiments and PST calculations at high C_6 values is consistent with the lack of centrifugal barriers for this dissociation, as discussed earlier. It is well known that exact calculations of the long-range potentials are difficult, especially in the absence of barriers [38], and large values were also used in the PST calculations for ketene [39]. Thus, we have used $C_6 = 10^{-76}$ J m^6 in all the calculations.

In our comparisons with statistical theories, we find that PST reproduces the rotational distributions much better than the "prior" statistical calculations [29]. In particular, the low J region in the NO(v=0) distributions, which deviates strongly from a linear Boltzmann plot (fig. 3), is reproduced only by PST. We note that PST conserves angular momentum and obeys detailed balance as opposed to prior statistical calculations, and the differences between prior calculation and PST are substantial for a small triatomic molecule such as NO_2 [29].

The PST calculations were carried out using an NO_2 parent rotational temperature of 10 K. Varying $T_{rot}(NO_2)$ between 2 and 20 K had little effect on the distributions [29]. The calculations are much more sensitive to the relative populations of the $O(^3P_J)$ spin–orbit states. These ratios have been found to vary nonmonotonically with photolysis energy, but in general are colder than statistical [7]. The general envelope of the NO rotational distributions is only slightly affected by varying the ratios of the $O(^3P_J)$ states. In contrast, the NO *vibrational* distributions are affected much more strongly. Suppressing the two upper $O(^3P_J)$ spin–orbit states increases the fraction of NO(v=1) by factors of 2–3 near the NO(v=1) threshold (fig. 4). The reason is simple. At E^+ near the v=1 threshold, only the $O(^3P_2)$ state is energetically available for NO(v=1) products, but all the $O(^3P_J)$ states are energetically available for NO(v=0). Eliminating the excited $O(^3P_J)$ states therefore will decrease the allowed fractional population in the NO(v=0) level without affecting the population of the NO(v=1) level.

4. Discussion

4.1. Energy distributions and statistical calculations

The NO rotational distributions determined in the 370 nm region are marked by fluctuations and structures in both v=0 and 1 which, particularly for v=0, are much larger than the experimental precision. These fluctuations are manifest in two forms. In the NO(v=1) distributions, which are limited to only a few rotational states, the populations of some levels are either abnormally high or low compared either to adjacent levels or to the predictions of PST. The corresponding NO(v=0) distributions show similar level-by-level fluctuations, but in addition broader structures are superimposed on an average that agrees fairly well with the predictions of PST (fig. 3). The general shapes of the expansion-cooled NO(v=1) distributions, as well as the existence of fluctuations, are very similar to the distributions observed in the photodissociation of expansion-cooled NO_2 near the threshold for NO(v=0) formation [2,29], and also near the threshold associated with the NO(v=0) + $O(^1D)$ channel [40]. In the latter case, the NO(v=0) distributions were obtained via a sequen-

tial two-photon photolysis using the mixed $1\,^2B_2/\tilde{X}\,^1A_1$ state as intermediate.

We find it remarkable, however, that despite the large fluctuations and superimposed structures, the rotational distributions cluster around an average that is well described by statistical theories. NO($v=0$) distributions obtained at $E^\dagger = 0$–1800 cm^{-1} behave similarly [29]. The statistical nature of the distributions has several manifestions: (i) the highest rotational level populated at each $E^\dagger$ corresponds to the highest level allowed energetically for dissociation of 7 ± 5 K NO_2; (ii) the observed thresholds for NO $v=0$ and 1 formations agree with their thermochemical values, as expected for dissociation without a barrier; and (iii) the average rotational energy increases monotonically with excess energy and no state-specific effects are observed at the excitation energies studied so far [29].

In contrast to the rotational distributions, the vibrational distributions do not agree with PST predictions from the onset of $v=1$. Not only do the $v=1$ populations exceed the PST predictions, but the relative $v=1$ population is somewhat larger at the lower excess energy. At $E^\dagger = 1949$ cm^{-1} (point A in fig. 2) $(v=1)/\sum v = 0.27 \pm 0.07$, while at $E^\dagger = 1998$ cm^{-1} (point B) the corresponding ratio is 0.20 ± 0.04. Previous studies have shown that at yet higher excess energies, the vibrational population of $v=1$ continues to rise, and at $\lambda \leqslant 351$ nm ($E^\dagger \geqslant 3360$ cm^{-1}), population inversion exists [1,2]. Thus, the NO vibrational populations are definitely dynamically controlled at the higher excess energies. It should be noted, however, that in other small molecules (e.g., NCNO [34]), the vibrational distributions near threshold are underestimated by PST, and other statistical theories (e.g., SSE [36], variational RRKM [40]) give better agreement with the experimental results. More data on the vibrational distributions as a function of excess energy are needed for more rigorous comparisons.

4.2. The mechanism of NO_2 dissociation: dynamics versus statistics

The results obtained in this work in conjunction with previous data suggest the following picture for the photodissociation of NO_2 at $E^\dagger \approx 2000$ cm^{-1}. Owing to the strong couplings between the optically accessible $1\,^2B_2$ state and the $\tilde{X}\,^2A_1$ state, the dissociation involves molecular eigenstates with a predominantly ground-state character [7,13]. However, the strong preferences for populating NO($v=1$) even near its threshold and NO($v>1$) at yet higher excess energies suggest that dynamical effects, which may originate in the conical intersection region, control the vibrational distributions. Recall that the conical intersection between the $^2B_2$ and $^2A_1$ states requires a vibration of b_2 symmetry (i.e. odd quanta of NO asymmetric stretch). In addition, at $E^\dagger > 1200$ cm^{-1} the unimolecular reaction lifetime is short, <0.5 ps, and thus intramolecular vibrational redistribution (IVR) may be incomplete. It appears that at $E^\dagger > 1900$ cm^{-1}, the initial parent NO-stretch excitation that promotes the crossing near the Franck–Condon region is preserved to some extent in the subsequent dissociation. In other words, the vibrational populations may be fixed early in the dissociation and their subsequent evolution is adiabatic, while the product rotational and translational distributions may be determined later along the reaction coordinate, at a transition state that is well described by PST.

We note that the products' electronic degrees of freedom are nonstatistical as well. NO($^2\Pi_{1/2}$) is favored over NO($^2\Pi_{3/2}$) compared with the statistical predictions [1–4,29], while the O($^3P_{2,1,0}$) spin–orbit components are colder than statistical for many wavelengths, and their relative populations show fluctuations as a function of excess energy [8]. If the vibrational and electronic states are correlated, then these fluctuations may lead to some fluctuations in the NO vibrational distributions as well, but more work to establish such correlations is needed.

The interpretation of the rotational distributions is more intriguing. On the one hand the distributions fit quite well, on the average, the predictions of PST, while on the other hand the fluctuations about the average are large and sensitive to the excess energy. Notice in particular the NO($^2\Pi_{1/2}$, $v=0$) distributions obtained at $E^\dagger = 1949$ and 1998 cm^{-1} (fig. 3). These two excess energies differ by only ≈ 50 cm^{-1} and should give rise to almost identical distributions. However, the populations of specific rotational levels can vary dramatically (e.g., large differences in the high J region).

We interpret the structures in the NO rotational distributions in terms of fluctuations around a statistical average for each final product state. Fluctuations in the partial cross sections into different final states were predicted theoretically in the decay of a strongly coupled compound nucleus, a process that is treated using statistical theories [42,43]. They were later observed in many nuclear reactions evolving via a compound nucleus and were termed "Ericson fluctuations" [43,44]. They arise when many overlapping resonances in the compound nucleus contribute to the product final states. In physical terms, it is well known that when two resonances in the excited complex overlap coherently, interferences in the product state distributions are expected. When many such resonances overlap, an exact theoretical treatment is unfeasible. In such cases, the transition matrix elements for the decay of the complex into different final states will have uncorrelated random phases, and therefore will give rise to fluctuations that are treated statistically [42,43]. In order to observe such fluctuations, the initial energy width should be less than the widths Γ of the resonances Γ should be greater than the average level spacings in the complex, and the density of final states should be low. For NO_2, it is well established that vibronic chaos exists even below dissociation threshold, and is manifest in strong fluctuations in the energy level spacings and fluorescence lifetimes [13,20]. Above dissociation threshold, the existence of rovibronic chaos has also been suggested [45]. These fluctuations have been analyzed using statistical treatments [13,20]. The overlaps between resonances will further increase above D_0 due to the increasing density and decay width of the activated complex levels. The averaging out of the fluctuations when summing over Λ-doublet NO levels and initial rotational states of NO_2 also suggests that the fluctuations are due to interference effects in the decay of states with overlapping resonances. It is also worth noting that random fluctuations in the unimolecular reaction rates of formaldehyde have been observed using Stark-shift measurements and rationalized with a statistical model [46].

To the best of our knowledge, this is the first time that Ericson fluctuations have been implicated in unimolecular decomposition. However, they may be present in the vibrational predissociation of other small systems with few degrees of freedom. For example, very recently Miller et al. studied the photodissociation dynamics of CO_2 at 157 nm, and reported that the $CO(X\,^1\Sigma^+, v=0, 1)$ rotational distributions corresponding to the $CO(X\,^1\Sigma^+) + O(^1D)$ channel also exhibit prominent structures, which are similar to those observed for NO_2 [47]. We therefore compared the CO distributions with PST predictions, using the same C_6 value as for NO_2 and the appropriate constants for CO. The results for CO $v=0$ and 1 are displayed in fig. 5 and show that the distributions are well described, on the average, by PST. It is thus possible that vibrational predissociation via an electronic state of CO_2 correlating with $CO(X\,^1\Sigma^+)+O(^1D)$ (e.g., the $^1B_2$ state) is responsible for the CO distributions. This interpretation is supported by the small recoil anisotropy, $\beta=0.0\pm0.4$ [47], which is consistent with lifetimes on the order of or larger than a rotational period. (The measured vibrational distribution, $(v=1)/\Sigma v$, is 0.21 ± 0.08 [45], as compared to 0.38 obtained by PST.) Another similarity between CO_2 and NO_2 dissociations involves the existence of conical intersections. Recent calculations show that, at least for linear geometries, the optically accessible valence states of CO_2 in the Franck–Condon region form conical intersections with Rydberg states [48].

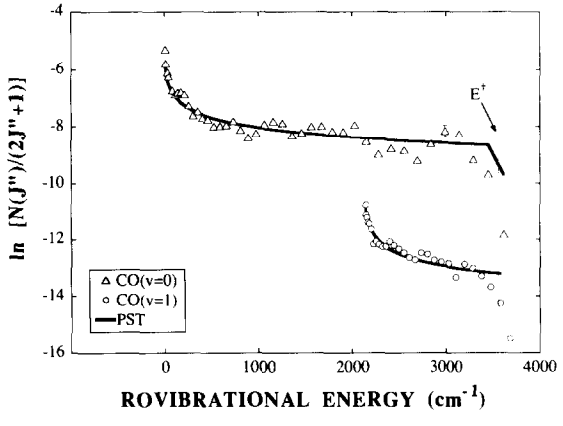

Fig. 5. Comparison between the $CO(v=0)$ (△) and $CO(v=1)$ (○) distributions obtained in the 157 nm photolysis of CO_2 by Miller et al. [44], and PST calculations (—). Arbitrary constants have been added to the results for each CO vibrational state for vertical separation. In the calculations a parent rotational temperature of 10 K was assumed. $E^\dagger$ marks the excess energy.

5. Summary

The photodissociation of NO_2 near the $NO(v=1)$ threshold was studied using a supersonic molecular beam. The vibrational distributions near the $v=1$ threshold are nonstatistical, and other work has shown that at higher excess energies vibrational population inversion exists. These distributions are probably controlled by dynamical effects which may originate in the region of the conical intersection between the $1\,^2B_2$ and $\tilde{X}\,^2A_1$ states.

The rotational distributions in both NO $v=0$ and 1 are described fairly well by PST and suggest that the decomposition of NO_2 at $\lambda \geqslant 370$ nm can be viewed as vibrational predissociation on the mixed $\tilde{X}\,^2A_1/1\,^2B_2$ surface. The pronounced structures in the rotational distributions cannot be explained within the framework of PST, and their source may be fluctuations in the partial cross sections into final states in the decay of a strongly coupled complex (i.e. many overlapping resonances). The apparent similarities between the product rotational distributions obtained in NO_2 and CO_2 photodissociations suggest the need for further theoretical studies to explore the connection between vibronic chaos and fluctuations in product state distributions, as well as the validity of statistical theories in describing these systems.

Acknowledgement

The authors wish to thank H.S. Taylor and R.W. Shaw for illuminating discussions on Ericson fluctuations, Y. Chen and C. Wittig for helpful discussions, P.L. Houston, I. Burak, K. Welge and R. Jost for communicating results prior to publication, and Leonard Pipes for assistance in data analysis. MH thanks the USC Chemistry Department for a Moulton Predoctoral Fellowship. This research was supported by the US National Science Foundation and the Army Research Office.

References

[1] H. Zacharias, M. Geilhaupt, K. Meier and K.H. Welge, J. Chem. Phys. 74 (1981) 218.

[2] H. Zaharias, K. Meier and K.H. Welge, in: Energy storage and redistribution in molecules, ed. J. Hinze (Plenum Press, New York, 1983).

[3] M. Mons and I. Dimicoli, Chem. Phys. Letters 131 (1986) 298.

[4] M. Mons and I. Dimicoli, Chem. Phys. 130 (1989) 307.

[5] H. Gaedtke and J. Troe, Ber. Bunsenges. Physik Chem. 79 (1975) 184;
H. Gaedtke, H. Hippler and J. Troe, Chem. Phys. Letters 16 (1972) 177.

[6] M. Quack and J. Troe, Ber. Bunsenges. Physik. Chem. 79 (1975) 469.

[7] G.A. Brucker, S.I. Ionov, Y. Chen and C. Wittig, to be published.

[8] J. Miyawaki, T. Tsuchizawa, K. Yamanouchi and S. Tsuchiya, Chem. Phys. Letters 165 (1990) 168;
J. Miyawaki, K. Yamanouchi and S. Tsuchiya, Chem. Phys. Letters 180 (1991) 287.

[9] E.A. Rohlfing and J.J. Valentini, J. Chem. Phys. 83 (1985) 521.

[10] M. Kawasaki, H. Sato, A. Fukuroda, T. Kikuchi, S. Kobayashi and T. Arikawa, J. Chem. Phys. 86 (1987) 4431.

[11] G.E. Busch and K.R. Wilson, J. Chem. Phys. 56 (1972) 3626, 3638.

[12] T. Suzuki, V.P. Hradil, S.A. Hewitt, P.L. Houston and B.J. Whitaker, Chem. Phys. Letters 187 (1991) 257.

[13] H. Köppel, W. Domcke and L.S. Cederbaum, Advan. Chem. Phys. 57 (1984) 59, and references therein.

[14] G.D. Gillispie and A.U. Khan, J. Chem. Phys. 65 (1976) 1624;
G.D. Gillispie, A.U. Khan, A.C. Wahl, R.P. Hosteny and M. Krauss, J. Chem. Phys. 63 (1975) 3425.

[15] G. Hirsch and R.J. Buenker, Can. J. Chem. 63 (1985) 1542;
G. Hirsch, R.J. Buenker and C. Petrongolo, Mol. Phys. 70 (1990) 835.

[16] C.F. Jackels and E.R. Davidson, J. Chem. Phys. 64 (1976) 2908; 65 (1976) 2941.

[17] L. Burnelle, A.M. May and R.A. Gangi, J. Chem. Phys. 49 (1968) 561;
R.A. Gangi and L. Burnelle, J. Chem. Phys. 55 (1971) 851.

[18] D. Hsu, D.L. Monts and R.N. Zare, Spectral atlas of nitrogen dioxide 5530 to 6480 Å (Academic Press, New York, 1978).

[19] K. Shibuya, T. Kusumoto, H. Nagai and K. Obi, J. Chem. Phys. 95 (1991) 720;
H. Nagai, K. Aoki, T. Kusumoto, K. Shibuya and K. Obi, J. Phys. Chem. 95 (1991) 2718.

[20] A. Delon and R. Jost, J. Chem. Phys. 95 (1991) 5686;
A. Delon, R. Jost and M. Lombardi, J. Chem. Phys. 95 (1991) 5701.

[21] E. Haller, H. Köppel and L.S. Cederbaum, J. Mol, Spectry. 111 (1985) 377;
Th. Zimmerman, H. Köppel and L.S. Cederbaum, J. Chem. Phys. 91 (1989) 3934.

[22] R.E. Smalley, L. Wharton and D.H. Levey, J. Chem. Phys. 63 (1975) 4977.

[23] A.E. Douglas and K.P. Huber, Can. J. Phys. 43 (1965) 74.

[24] U. Robra, H. Zacharias and K.H. Welge, Z. Physik D 16 (1990) 175.
[25] C.H. Chen, D.W. Clark, M.G. Payne and S.D. Kramer, Opt. Commun. 32 (1980) 391.
[26] R.J.S. Morrison and E.R. Grant, J. Chem. Phys. 77 (1982) 5994.
[27] D. Proch and J. Trickl, Rev. Sci. Instr. 60 (1989) 713.
[28] D.C. Jacobs and R.N. Zare, J. Chem. Phys. 85 (1986) 5457; D.C. Jacobs, R.J. Madix and R.N. Zare, J. Chem. Phys. 85 (1986) 5469.
[29] M. Hunter, D.C. Robie and H. Reisler, to be published.
[30] I. Deézsi, Acta Phys. Hung. 9 (1958) 125.
[31] D.C. Jain and R.C. Sahni, Trans. Faraday Soc. 64 (1968) 3169;
H. Scheingraber and C.R. Vidal, J. Opt. Soc. Am. B 2 (1985) 343.
[32] A. Lagerqvist and E. Miescher, Helv. Phys. Acta 31 (1958) 221;
R. Engleman, P.E. Rouse, J.M. Peek and V.D. Baimonte, Los Alamos Laboratory Scientific Report LA 4364 (1970);
P.A. Freedman, Can. J. Phys. 55 (1977) 1387;
C. Amiot, R. Bacis and G. Guelachvili, Can. J. Phys. 56 (1982) 251;
C. Amiot and J. Verges, Physica Scripta 25 (1982) 302.
[33] P. Pechukas and J.C.Light, J. Chem. Phys. 42 (1965) 3281;
[34] P.C. Pechukas, C. Rankin and J.C. Light, J. Chem. Phys. 44 (1966) 794.
[35] J.C. Light, Faraday Discussions Chem. Soc. 44 (1967) 14.
[36] H. Reisler, M. Noble and C. Wittig, in: Molecular photodissociation dynamics, ed. J. Baggot and M.N.R. Ashfold (Roy. Soc. Chem., London, 1987) p.139.
[37] W. Forst, Theory of unimolecular reactions (Academic Press, New York, 1973);
R.D. Levine and R.B. Bernstein, Molecular reaction dynamics and chemical reactivity (Oxford Univ. Press, Oxford, 1987).
[38] J. Troe, in: Mode selective chemistry, eds. J. Jortner, R.D. Levine and B. Pullman (Kluwer, Dordrecht, 1991), and references therein.
[39] I.-C. Chen, W.H. Green Jr. and C.B. Moore, J. Chem. Phys. 89 (1988) 314.
[40] L. Bigio and E.R. Grant, J. Phys. Chem. 89 (1985) 5855; J. Chem. Phys. 87 (1987) 360.
[41] S.J. Klippenstein, L.R. Khundkar, A.H. Zewail and R.A. Marcus, J. Chem. Phys. 89 (1988) 4761.
[42] T. Ericson, Phys. Rev. Letters 5 (1960) 430.
[43] P.E. Hodgson, Nuclear reactions and nuclear structure (Clarendon Press, Oxford, 1971).
[44] R.W. Shaw, J.C. Norman, R. Vandenbosch and C.J. Bishop, Phys. Rev. 184 (1969) 1040.
[45] R. Jost, private communication.
[46] W.F. Polik, D.R. Guyer, W.H. Miller and C.B. Moore, J. Chem. Phys. 92 (1990) 3471.
[47] R.L. Miller, S.H. Kable, P.L. Houston and I. Burak, J. Chem. Phys. 96 (1992) 32.
[48] P.L. Knowles, P. Rosmus and H.-J. Werner, Chem. Phys. Letters 146 (1988) 230;
A. Spielfiedel, N. Feantrier, G. Chambaud, P. Rosmus and H.-J. Werner, Chem. Phys. Letters 183 (1991) 16.